Journal of Solid State Chemistry 181 (2008) 2731–2736

Contents lists available at ScienceDirect

Journal of Solid State Chemistry

journal homepage: www.elsevier.com/locate/jssc

How isopolyanions self-assemble and condense into a 2D tungsten oxide crystal: HRTEM imaging of atomic arrangement in an intermediate new hexagonal phase

A. Chemseddine *, U. Bloeck

Helmholtz-Zentrum Berlin für Materialien und Energie GmbH, Solarenergieforschung SE4, Glienicker Str. 100, 14109 Berlin, Germany

ARTICLE INFO

Article history:
Received 5 May 2008
Received in revised form
2 July 2008
Accepted 6 July 2008
Available online 11 July 2008

Keywords:
Isopolytungstic acid
Tungsten oxide
Structure
HRTEM
Sol–gel

ABSTRACT

The structure and structural evolution of tungstic acid solutions, sols and gels are investigated by high-resolution electron microscopy (HRTEM). Acidification of sodium tungstate solutions, through a proton exchange resin, is achieved in a way that ensures homogeneity in size and shape of intermediate polytungstic species. Gelation is shown to involve polycondensation followed by a self-assembling process of polytungstic building blocks leading to sheets with a layered hexagonal structure. Single layers of this new metastable phase are composed of three-, four- and six-membered rings of WO_6 octahedra located in the same plane. This is the first time that a 2D oxide crystal is isolated and observed by direct atomic resolution. Further ageing and structural evolution leading to single sheets of 2D ReO_3-type structure is directly observed by HRTEM. Based on this atomic level imaging, a model for the formation of the oxide network structure involving a self-assembling process of tritungstic based polymeric chain is proposed. The presence of tritungstic groups and their packing in electrochromic WO_3 films made by different techniques is discussed.

1. Introduction

Electrochromic tungsten oxide was investigated considerably for its use as thin films in display devices and smart windows. The performance of these devices depends strongly on the oxide structure and microstructure. However, despite extensive structural studies on films made by solution, sol–gel as well as by gas phase techniques, the packing of WO_6 octahedra in these film is still not elucidated.

Solution chemists were able to identify and characterize different intermediate polymeric species in solution. However, it is not clear how these species, which exhibit different atomic packing, are involved in the formation of extended and less dense oxide structures [1–3].

Fig. 1 shows, on one hand, the different structures of well-characterized isopolytungstic species formed in solution after acidification of tungstate [4] and on the other hand, the structure of the final hydrated oxide which precipitates as a solid on lowering the pH [5,6]. The last species which was identified as the starting point for further polymerization was called ψ' metatungstic acid which is a protonated form of the so-called ψ metatungstic acid [3,4,7,8]. These species were suggested to be polymeric and consist of compact W_3O_{13} groups but with ill-defined degrees of condensation owing to their instability [3] tetramers of $W_6O_{19}^{2-}$ were also suggested by Lemerle and Lefebvre to form this acid which is called α [9].

At higher tungsten concentrations, sols then gels are formed before precipitation of the crystalline phase $WO_3 \cdot 2H_2O$ [6] At the sol–gel transition, tungsten oxide films can be processed by spin-coating and investigated for their electrochromic properties [10]. The performances of tungsten oxide films as active electrodes in display devices depends strongly on the structure and microstructure of the oxide films [11–13]. Therefore, the need to understand the structural evolution of tungstic acid during the sol–gel transition and formation of the extended oxide network is also of great importance from the point of view of applications.

By using X-ray diffraction measurements and analysis of the pair distribution functions (PDFs), Nanba and Yasui were able to extract interesting structural information for films made by physical [14] as well as by sol–gel method similar to the present study [15]. The authors did propose microcluster models for these films by comparing the observed PDFs with those calculated for hexagonal WO_3 and $WO_3 \cdot 1/3H_2O$. The framework structures of these films was suggested to consist of clusters in which the octahedra are similarly packed as in hexagonal WO_3 (2–3). A similarity in the structure between both films was found except for the presence of edge-sharing WO_6 octahedra in the films made by wet chemistry [14,15].

* Corresponding author. Fax: +49 30 80622434.
E-mail address: chemseddine@hmi.de (A. Chemseddine).

0022-4596/$ - see front matter © 2008 Elsevier Inc. All rights reserved.
doi:10.1016/j.jssc.2008.07.001

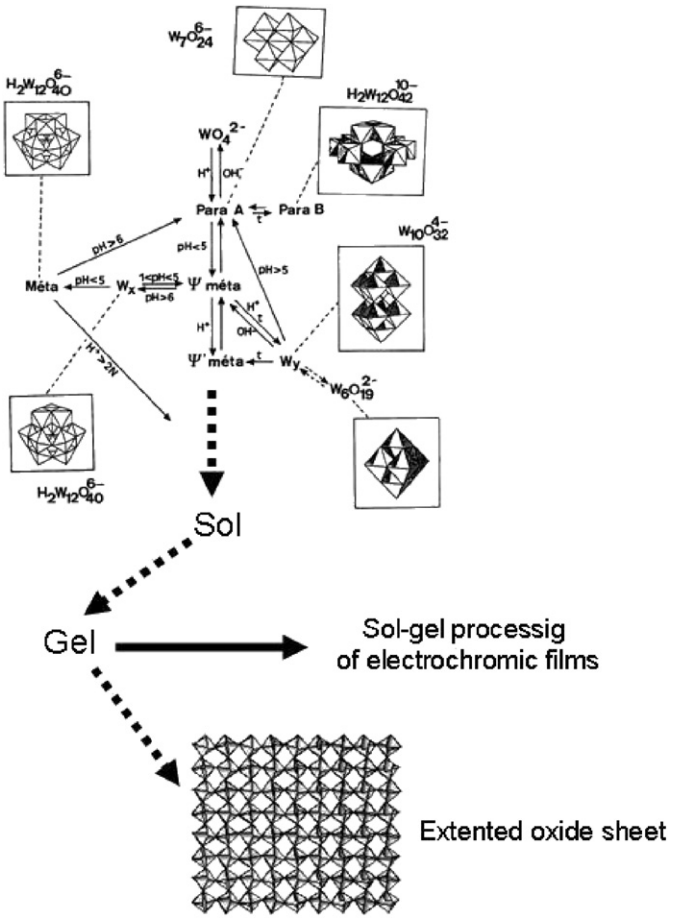

Fig. 1. Scheme showing tungstate pH dependent polymerization. The structures of some isolated isopolytungstates and a model structure of the final precipitate.

The major obstacle to structural investigations of these amorphous oxides films is the distribution in structure, size and shape of the polytungstic species and their ways to polymerize and aggregate during film formation. Therefore, efforts were directed to providing homogeneous precursor solutions.

The great advantage of monosized species is their propensity to self-assemble leading to ordered and relatively stable structures. In this case, higher quality structural data can be obtained due to the films stability and larger correlation length. Such high homogeneity will open the door for the tailoring of film structure and microstructure. This offers the unique opportunity to synthesize homogenous films of different packing orders and examine directly their electrochromic properties.

A previous ionic exchange method [3,10] was modified to synthesize highly homogenous tungstic acid solutions and organized gels and films. High-resolution electron microscopy (HRTEM) was the main technique used to extract information at the atomic level on the structure and structural evolution of these tungsten oxide networks.

The synthesis and TEM sampling provide extremely thin specimens leading to micrographs with a high and correct contrast. The electron beam suffers little loss as multiple scattering is minimized, these specimen can therefore be considered as phase objects. If the images are taken at the so-called Scherzer defocus, the image contrast reflect the two-dimensional arrangement of atoms [16].

Since the basic unit in theses systems is the WO_6 octahedra as shown in Fig. 1, the structural evolution during the sol–gel transition and the gel ageing involve changes in modes of linkage between octahedra and therefore to changes in W–W distances. The measurement of these distances directly on the HRTEM pictures and the use of existing knowledge in structural chemistry allow a satisfactory interpretation of these structures without the need for image simulation [16].

2. Experimental

Ion exchange reactions were achieved by passing an aqueous sodium tungstate solution (0.5 mol/l) through a column filled with a proton resin (Lewatit) [3,10]. Tungstic acid solutions are obtained drop-by-drop at the bottom of the column creating differences in growth stages between cluster populations and therefore a distribution in size, shape and structure. In this investigation, exchange reaction is achieved by mixing sodium tungstate solution with a portion of a given quantity of resin under strong stirring, then filtered quickly under vacuum and mixed with the next fresh resin portion. This procedure was repeated three times. A clear yellow solution is obtained which transforms in about an hour into a transparent yellow gel. During this ageing of solutions, sols and gels, portions were taken and investigated by HRTEM.

HRTEM observations were performed using a Philips CM12 microscope with an accelerating voltage of 120 kV and equipped with a super twin lens. Tungstic acid colloids and gels were deposited a plasma-etched amorphous carbon substrates with thickness between 20 and 60 Å.

3. Results

Fig. 2 shows a series of TEM images recorded during the evolving sol–gel transition of tungstic acid, during the shrinkage (syneresis process) and just before precipitation. These are the steps where major structural changes were observed.

Fig. 2A shows a low magnification TEM micrograph during gelation. After water evaporation, the dried gel consists of a continuous three-dimensional network of colloidal particles or aggregates with dimensions around 10 ± 1 nm in diameter.

At relatively high resolution, Fig. 2B, these aggregates are themselves formed of smaller almost spherical monosized clusters with a diameter of around 1 nm. These smaller units, which have a size within the range of an isopolytunstate like decatungstate or metatungstate form a much more compact structure. Attempts to obtain HRTEM images were difficult due to the instability of the particles under the electron beam.

Fig. 2C shows a HRTEM of the gel before any shrinkage and syneresis. Arrows indicate elongated small clusters with a thickness around 3 ± 0.3 Å and a distribution in length between 4 and around 18 Å. Arrows 1 and 2 point to clusters which show clearly a corrugated structure with segment length between 4 and 6 Å. These units self-assemble parallel to each other as shown by arrows shown in Fig. 2C. At this stage, no significant long range ordering was observed. In addition, the clusters and the structures investigated seem to be unstable during HRTEM observations.

After 1 day of ageing the gel expels water and begins to exhibit a lamellar structure. In addition, the sheets observed are well organized and relatively stable allowing us to record high-resolution images. Fig. 2D shows a HRTEM micrograph of polytungstic building blocks stacked in sheets. These building units have a diameter of about 1 nm. The electron diffraction pattern reveals a hexagonal phase with $a = b = 10 \pm 0.5$ Å. Arrows point to structural changes at the edges of the sheets. This can be induced by dilution required for the TEM sampling or the beginning of the next restructuration of the sheet.

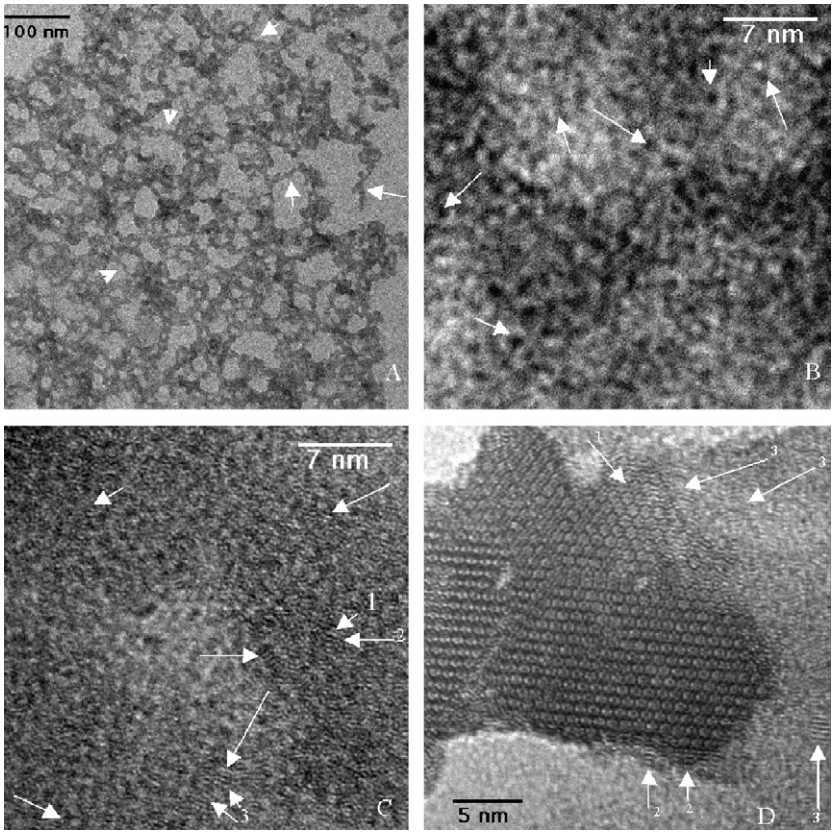

Fig. 2. TEM micrographs taking during the tungstic acid sol–gel transition. (A and B) just after gelation, (C) just before shrinkage and syneresis and (D) 1 day of shrinkage.

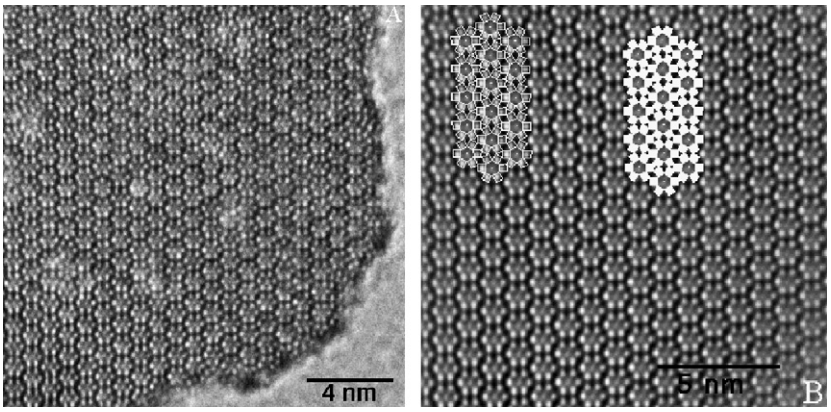

Fig. 3. Original HRTEM of a single sheet taking just before precipitation. The same image after Fourier filtering of the noise and a structural model for the new metastable hexagonal phase.

At this stage of evolution some sheets are relatively stable allowing HRTEM imaging of a new intermediate metastable structure of the sheet. In Fig. 3, white spots are arranged in a regular manner and the measured distances between two adjacent spots are 3.33, 3.70 Å and 4.07 ± 0.2 Å corresponding, respectively, to adjacent points in six-, four- and three-membered rings. These distances correspond to the W–W distance where the WO_6 octahedra are sharing vertices. The extracted distances between other tungsten neighbors allows a direct correlation between image contrast and the structure of this intermediate phase. The structure can be described as octahedra stacked in sheets, sharing corners and arranged in three-, four- and six-membered rings. A filtered image and a constructed structural model of this new hexagonal phase is illustrated in Fig. 3.

In previous investigations, multiple stacked sheets were observed at low magnification. It was not possible to take high-resolution micrographs due to the tendency of these multiple sheets to roll under the electron beam leading to objects similar to tubes. However, the single sheet of Fig. 3 shows a great stability during TEM observation. This can probably be explained by the difference in strength of the interaction of single sheet with the substrate and sheet–sheet interaction.

Fig. 4A shows HRTEM micrographs of another single sheet. Arrows point to the appearance of two adjacent four-membered rings in the middle of the sheet as well as others on the edges. This packing is illustrated by a model in Fig. 4B.

Fig. 5 shows the breakdown of the hexagonal phase into smaller polytungstic species leading finally to the pure

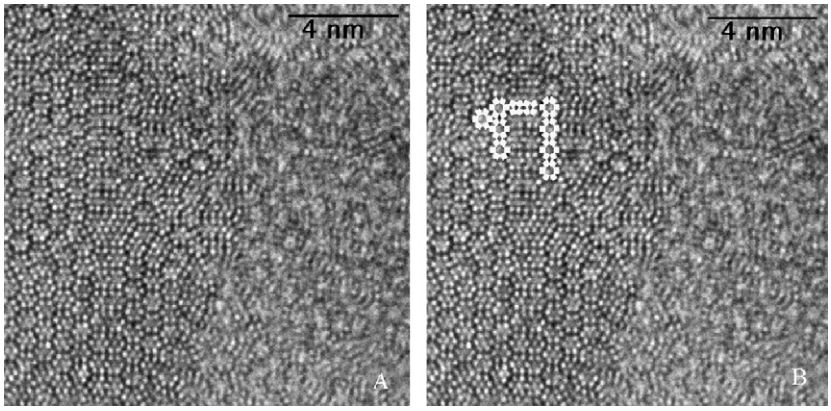

Fig. 4. HRTEM of a single sheet with an arrow pointing to two adjacent four-membered rings. This packing is shown by a model in (B).

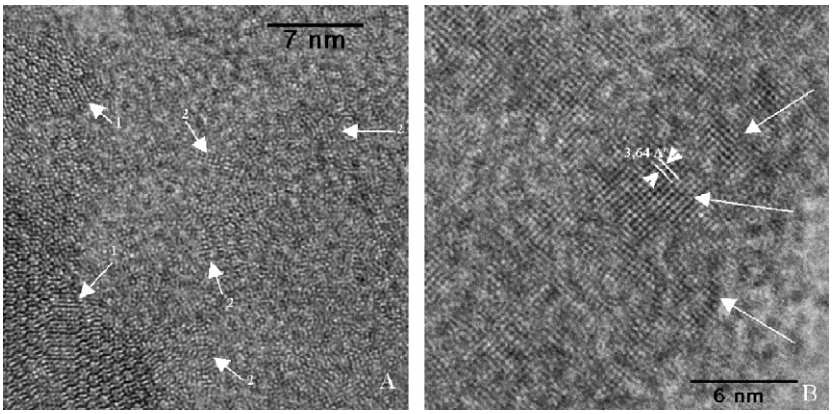

Fig. 5. (A) Arrows point to many small clusters during the breakdown of the hexagonal phase and (B) pure four-membered rings phase observed in the final precipitate.

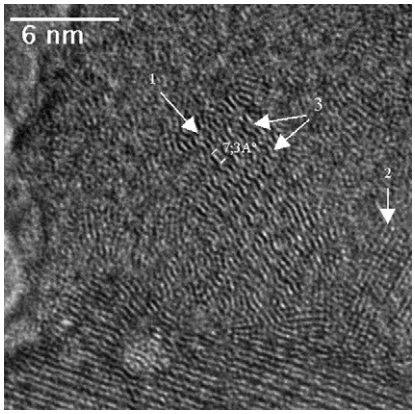

Fig. 6. HRTEM of stacked sheets during breakdown and precipitation. Arrows point to corrugated chains.

four-membered rings phase. This step illustrates the precipitation process to the final oxide hydrate shown in Fig. 5.

These tungstic acids gels are known for their instability. Gel contraction and syneresis processes are followed by precipitation of layered tungsten oxides hydrates with the general formula $WO_3 \cdot 1H_2O$ or $WO_3 \cdot 2H_2O$ hydrates. The structure of these oxides consists of octahedra arranged in infinite layers linked by vertices and forming exclusively four-membered rings [5,6] (Fig. 1).

Fig. 6 shows the precipitation and breakdown of the hexagonal phase in a relatively concentrated sample where stacked multi-sheets were observed. Arrow 3 points to the detachment through hydrolysis of corrugated chains while arrow 2 points to structures where only four-membered rings are observed. In the case of stacked sheets, the contrast is relatively poor compared to Figs. 3 and 4.

4. Discussion

A close inspection of the HRTEM images shows that in many cases and at a given evolution stage of the gel, single sheets of tungstic acid gel were successfully deposited on carbon substrates during TEM sampling. In contrast to multi-sheet specimens, single sheets were relatively stables for HRTEM observation. The comparison between Figs. 3 and 4 also suggest that the objects observed are in fact single sheets. The contrast shown by the four-membered ring indicated by arrow in Fig. 4 suggests the absence of others sheet below. Furthermore, during TEM observation, detachment of small and individual clusters from the sheet edge shows no presence of other sheets below either but only features of carbon substrate. This also true for the final precipitate observed in Fig. 5 where only 2D packing is observed.

However, during HRTEM observations of multi-sheets samples, changes and instability of the specimen were observed. In addition to the lack of adherence of stacked sheets to the carbon substrate, the sheets roll under the beam heat leading to objects like tubes or needles and sometimes to particles with undefined shapes.

The thermodynamic stability of these single sheets which can be seen as 2D crystals can be explained by the bonding and coordination of tungsten atoms in these sheets. The sheet is built

up from layers of corner sharing $WO_5(H_2O)$ octahedra, each tungsten is surrounded by one terminal oxygen Ot along the direction normal to the sheet, four bridging oxygen Ob in the sheet plane and one water molecule at the opposite position to the W═O short bond. This coordination remains, in fact, in the final precipitates $WO_3 \cdot 2H_2O$ and $WO_3 \cdot 1H_2O$ [5,6] where octahedra form only four-membered ring. According to many infrared and Raman studies on tungstic acid solutions and gels, the terminal bond W═O present in isopolytungstates, remains during all the process of ageing [17–19]. According to Taube and Ballhausen, this bonding is energetically favorable [20].

To explain the formation of the 2D crystal shown in Fig. 3, a model is proposed (Fig. 7) by assuming $W_3O_6(OH)_6(H_2O)_3$ as the primary building unit. These units can condense by eliminating two water molecules and forming $W_6O_{14}(OH)_8(H_2O)_6$ containing the four-membered ring. Further condensation of these species leads to tritungstic chains of general formula $W_{3(n+1)}O_{6+8n}(OH)_{6+2n}(H_2O)_{3(n+1)}$ ($n = 0, 1, 2$, etc.).

According to an ultracentrifugation experiment (mass not given) the cluster with 24 atoms mentioned in Lemerle's work would have $W_{24}O_{62}(OH)_{20}(H_2O)_{24}$ [9] as a possible formula. In a previous study of ψ metatungstate, the formula $[W_{24}O_{72}(OH)_{12}]^{12-}$ was attributed to the mass found by the same technique. This anion will correspond to a neutral species $W_{24}O_{62}(OH)_{20}(H_2O)_2$ in aqueous solution.

In the freshly prepared solution, hexatungstate and decatungstate isopolyanions were also identified by ^{183}W and other techniques [17,21]. These species were shown to transform into metatunstic acid consisting of compact trititungstic groups [3,18]. Our observations suggest that acid catalyzed hydrolysis as shown in Fig. 8, will lead to $W_{3(n+1)}O_{6+8n}(OH)_{6+2n}(H_2O)_{3(n+1)}$ type chains.

The condensation kinetics of these tritungstic groups through formation of four-membered rings and the length of the corrugated chains obtained depend on the overall tungsten concentration (pH in this case) and on the presence of other cations if acidification is achieved through acid addition. This will explain the differences in degree of aggregation found for these species by different authors. Six-fold was found by salt cryoscopy [22], 12 by sedimentation equilibrium technique [23] and 24-aggregation was found by ultracentrifugation [24]. The present HRTEM observations indicate the propensity of these groups to further condense into chains which in turn self-assemble and condense in a 2D oxide with four- and six-membered rings as shown in Fig. 9.

Removal of solvent during the sol–gel processing of films leads to the stabilization of this phase. These films are generally made from fresh solutions, containing a mixture of tungstic species. Aggregation and condensation processes are accelerated during spin-coating. Additional structural development and mass transfer take place during heat-treatment and water elimination. The structure of these films was found to be similar to films made by evaporation techniques [14,15]. It is important to mention that both types of films undergo structural evolution in high humidity atmosphere leading to the same final and stable crystalline phase $WO_3 \cdot 2H_2O$ [5,25]. At high temperatures, Berkowitz et al. [26] identified W_3O_9, W_4O_{12} and W_5O_{15} as polymeric species formed in the gas phase by mass spectrometry. The landing of these clusters on a cold solid substrate leads to amorphous tungsten oxide films. Decades ago, the presence of tritungstic groups in these films was postulated by Arnoldussenn by investigating the effect of water and analyzing dissolution products. He suggested a molecular solid model composed of W_3O_9 trimers stabilized by water molecules [27].

In their structural study of both types of films, Nanba et al. were able to identify the presence of three-, four-, and six-membered rings, however their technique is limited in extracting distances for pairs of tungsten atoms. Their model is based on comparison with only the known tungsten oxide phases [28].

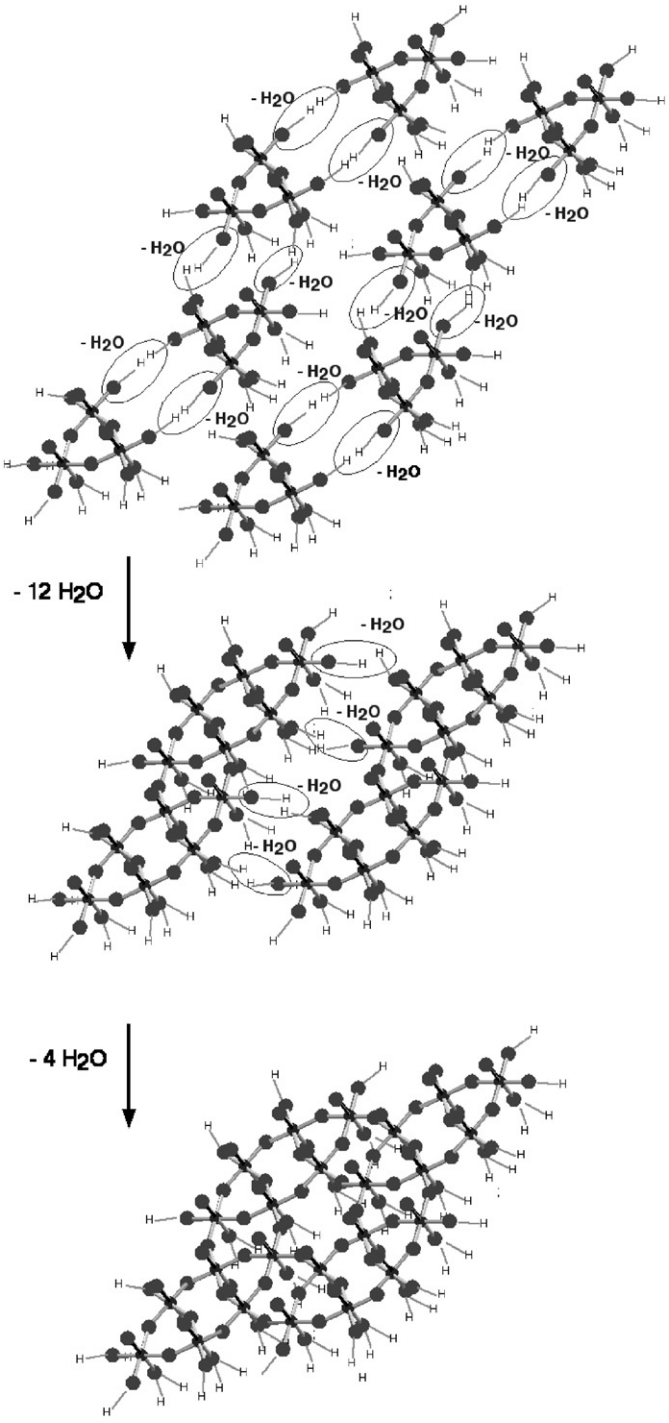

Fig. 7. Schematic, proposed structure for $W_3O_6(OH)_6(H_2O)_3$ tritungstic groups as basic units and their condensation processes leading to corrugated chains then to sheet.

The direct atomic imaging of the 2D hexagonal phase shown in Fig. 3 and the formation mechanism discussed in this work indicate three important findings. (a) Primary building unit for electrochromic tungsten oxide are planar tritungstic groups where three octahedra share vertices forming a three-membered ring. (b) These units prefer to condense forming corrugated chains

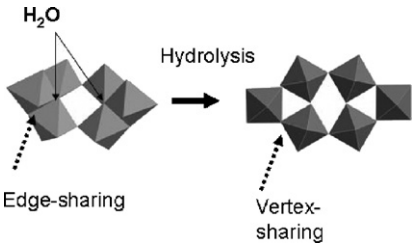

Fig. 8. Schematic, transformation of compact tritungstic groups (edge-sharing octahedra) by hydrolysis to tritungstic groups with only vertexes sharing octahedral.

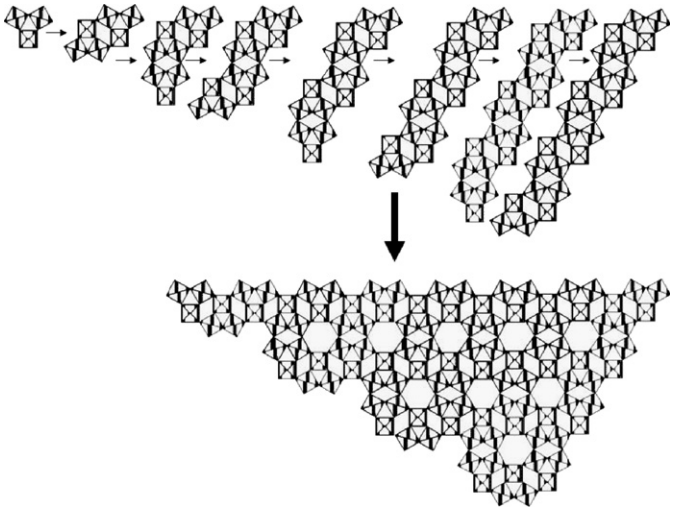

Fig. 9. Schematic, proposed polyhedral model for $W_3O_6(OH)_6(H_2O)_3$ tritungstic groups as basic units and their condensation processes leading to 2D hexagonal crystal.

with only four-membered rings. These chains condense into two-dimensional structure leading to four- and six-membered rings.

Depending on the techniques and on the preparations conditions variations in structures and microstructures, depend on the populations of clusters landing on the substrate and their way of aggregation or condensation. The building up of the oxide network is very sensitive to moisture and oxygen concentration. This will determine the atomic packing, cluster or particles sizes and therefore the electrochromic properties. This study shows the metastabililiy of these intermediate phases. Water attack network bond (hydrolysis) leading to dissolution, restructuration and crystallization. The high concentration of water present in pores and between sheets explains the high kinetics compared to xerogel films or evaporated films.

5. Conclusion

The structural evolution of tungstic acid solution during the sol–gel transition, gel ageing and finally during precipitation using HRTEM is shown. The direct imaging of the clusters which self-assemble into a new intermediate hexagonal phase was achieved. The clusters with the formula $W_3O_6(OH)_6(H_2O)_3$ condense into corrugated chains leading to 2D crystals. These stacked 2D crystals exfoliated during TEM sampling allowing, for the first time, atomic imaging of a 2D oxide crystal. The structural evolution and the precipitation to the known oxide hydrate are successfully imaged. It is clearly shown that on one hand, the local structure in the gel is different from the precipitate. On the other hand, the packing of the octahedra is different from most isopolyanions and most tungsten oxide phases identified to date. A new metastable phase was made and identified by controlling the homogeneity of the precursor solutions. Finally, a formation mechanism is proposed.

Acknowledgments

The authors thank the Helmholtz-Zentrum Berlin für Materialien und Energie GmbH for financial support.

References

[1] J. Livage, M. Henry, C. Sanchez, Prog. Solid State Chem. 18 (1988) 259–348.
[2] M. Henry, J.P. Jolivet, J. Livage, J. Struct. Bond. 77 (1991) 153–206.
[3] A. Chemseddine, M. Henry, J. Livage, J. Rev. Chim. Miner. 21 (1984) 487.
[4] M.T. Pope, Heteropoly and Isopolyoxometallates, Springer, Berlin, Heidelberg, New-York, 1983.
[5] A. Chemseddine, F. Babonneau, J. Livage, J. Non Cryst. Solids 91 (1987) 271.
[6] T. Szymanski, Can. Mineral. 22 (1984) 681–688.
[7] P. Souchay, M. Boyer, Chauveau. Trans. R. Inst. Technol. Stockholm 259 (1972) 161.
[8] O. Glemser, W.Z. Holtji, W. Naturforsch. 20b (1965) 75.
[9] J. Lemerle, J. Lefebvre, Can. J. Chem. 55 (1977) 3758–3762.
[10] A. Chemseddine, R. Morineau, J. Livage, Solid State Ionics 5 (10) (1983) 357.
[11] C.G. Granqvist, Appl. Phys. A 57 (1993) 3–12.
[12] J.P. Cronin, D.J. Tarico, J.C.L. Tonazzi, A. Agrawal, S.R. Kennedy, Sol. Energy Mater. 29 (1993) 387.
[13] H.R. Zeller, H.U. Beyeler, Appl. Phys. 13 (1977) 231–237.
[14] T. Nanba, I. Yasui, J. Solid State Chem. 83 (1989) 304–315.
[15] T. Nanba, Y. Nishiyama, I. Yasui, J. Mater. Res. 6 (1991) 1324–1333.
[16] L. Eyring, in: P.R. Buseck, J.M. Cowley, L. Eyring (Eds.), High-Resolution Transmission Electron Microscopy and Associated Techniques, Oxford University Press, New York, Oxford, 1988.
[17] A. Chemseddine, These de Doctorat d'Etat Université Pierre et Marie Curie ParisVI, Juin 1986.
[18] S. Baldilescu, M. Minh-Ha, G. Bader, P.V. Ashrit, F.E. Girouard, V.-V. Truong, J. Mol. Struct. 297 (1993) 393–400.
[19] A. Takase, K. Miyakawa, Jpn. J. Appl. Phys. 30 (1991) L1508.
[20] J.C. Goloboy, W. Klemperer, T.A. Marquart, G. Westwood, O.M. Yaghi, Nato Csi. Ser. II 98 (2003) 79–174;
C.J. Ballhausen, H.B. Gray, Inorg. Chem. 1 (1962) 111–122;
H. Taube, Chem. Rev. 50 (1952) 69–126.
[21] A. Chemseddine, C. Sanchez, J. Livage, J.P. Launay, M. Fournier, Inorg. Chem. 23 (1984) 2609–2613.
[22] P. Souchay, Ann. Chim. 18 (1943) 61;
P. Souchay, Ann. Chim. 18 (1943) 73;
P. Souchay, Ann. Chim. 18 (1943) 169.
[23] M. Boyer, P. Souchay, Rev. Chim. Miner. 8 (1971) 591.
[24] O. Glemser, W. Holznagel, W. Höltje, E. Schwartzmann, Z. Naturforsch. B 20 (1965) 725.
[25] N. Yoshiike, S. Kondo, J. Electrochem. Soc. 131 (1984) 809–812.
[26] J. Berkowitz, W.A. Chupka, M.G. Ingham, J. Chem. Phys. 27 (1957) 85.
[27] T.C. Arnoldussen, J. Electrochem. Soc. 128 (1981) 117.
[28] M. Figlarz, Prog. Solid State Chem. 19 (1989) 46.